Mechanisms of flecainide induced negative inotropy: An in silico study

Pei-Chi Yang[a,*], **Wayne R. Giles**[c], **Luiz Belardinelli**[b], **Colleen E. Clancy**[a,*]

[a]Department of Physiology and Membrane Biology, School of Medicine, University of California, Davis, United States of America

[b]InCarda Therapeutics, Newark, CA, United States of America

[c]Department of Physiology & Pharmacology, University of Calgary, Canada

Abstract

It is imperative to develop better approaches to predict how antiarrhythmic drugs with multiple interactions and targets may alter the overall electrical and/or mechanical function of the heart. Safety Pharmacology studies have provided new insights into the multi-target effects of many different classes of drugs and have been aided by the addition of robust new in vitro and in silico technology. The primary focus of Safety Pharmacology studies has been to determine the risk profile of drugs and drug candidates by assessing their effects on repolarization of the cardiac action potential. However, for decades experimental and clinical studies have described substantial and potentially detrimental effects of Na^+ channel blockers in addition to their well-known conduction slowing effects. One such side effect, associated with administration of some Na^+ channel blocking drugs is negative inotropy. This reduces the pumping function of the heart, thereby resulting in hypotension. Flecainide is a well-known example of a Na^+ channel blocking drug, that exhibits strong rate-dependent block of I_{Na} and may cause negative cardiac inotropy. While the phenomenon of Na^+ channel suppression and resulting negative inotropy is well described, the mechanism(s) underlying this effect are not. Here, we set out to use a modeling and simulation approach to reveal plausible mechanisms that could explain the negative inotropic effect of flecainide. We utilized the Grandi-Bers model [1] of the cardiac ventricular myocyte because of its robust descriptions of ion homeostasis in order to characterize and resolve the relative effects of QRS widening, flecainide off-target effects and changes in intracellular Ca^{2+} and Na^+ homeostasis. The results of our investigations and predictions reconcile multiple data sets and illustrate how multiple mechanisms may play a contributing role in the flecainide induced negative cardiac inotropic effect.

*Corresponding authors at: Davis Campus Office, Davis Campus Lab, Tupper Hall, RM 4303, Davis, CA 95616-8636, United States of America. ceclancy@ucdavis.edu (C.E. Clancy).

Keywords

Flecainide; Ion channel; Pharmacology; Safety pharmacology; Cardiac inotropy

Subject codes

Inotropy; Electrophysiology; Computational biology; Pharmacology

1. Introduction

While important progress has been made recently via safety pharmacology studies designed to screen drugs for pro-arrhythmia, the primary focus has been on determining the extent to which drugs cause repolarization abnormalities [1,2]. In particular, the emphasis has been on the proclivity for drugs to block the cardiac potassium channel hERG, an infamously promiscuous drug target [3-5]. More recently, studies have begun to take into account the simultaneous effects of drugs on multiple cardiac ion channel. These usually result in complex nonlinear emergent dynamics that can alter the electrophysiological behavior in the heart in unpredictable ways [2]. Computational modeling and simulation approaches have proven to be a useful complement to experimental studies in attempts to rationalize and predict the complex ion channel blocking drug effects on normal cardiac physiology and in pathological states associated with disease.

The focus on repolarization abnormalities in safety pharmacology screening has resulted in insufficient emphasis on closely related depolarization abnormalities and the potential side effects resulting from inhibition of sodium current, although some new technologies are emerging [6]. Such side effects include well-known conduction slowing, but in the ventricle other side effects are also recognized as important risk factors for drug safety [7-10]. One such example is the potential for some sodium channel blocking drugs to reduce the effective mechanical functioning of the heart via a reduction in inotropy, thereby resulting in substantial reduction in the effective pumping function of the ventricles [11,12].

Experimental data obtained from multiple species and from clinical studies have consistently demonstrated a significant negative inotropic effect of flecainide within the clinically relevant dosing range. This strongly contraindicated phenotype is heart rate dependent and exacerbated by rapid heart rate as well in the ischemic and failing heart [8,9,13-20].

Here we have developed a computational framework to predict Na^+ channel drug effects on normal cardiac electrophysiology in the Grandi-Bers computational representations of ventricular [21] myocytes and tissue. We have revealed the effects of flecainide on key parameters that regulate cardiac inotropy resulting in new insights regarding Na channel blocker induced negative inotropy. Here we explore the reported plasma concentration ranges reported in humans to assess the physiological relevance and mechanisms of flecainide induced negative inotropy. The therapeutic plasma range of 0.5 to 2.4 μM Flecainide corresponds to administration of ~200 to 1000 ng/mL [22,23].

2.   Methods

We utilized the computational models based on the Grandi-Bers formulations for atrial [24] and ventricular [21] myocyte action potential and [Ca^{2+}] homeostasis as well as the O'Hara-Rudy ventricular human model [25]. The computational model for flecainide interaction with the cardiac Na$^+$ channel is based on publications from the Clancy Group [26,27], with flecainide interaction with the RyR2, I$_{Kr}$, I$_{to}$, and I$_{CaL}$ informed by our simulation studies and experimental data [1,27-29].

2.1.   RyR2 – flecainide drug-channel interaction model

The Shannon-Bers Markov model formulation of the RyR2 [30] was modified to include a drug bound state *DO* with transitions k$_{on}$ = D* [Drug] and k$_{off}$ = D*IC$_{50,Drug}$ to and from the open state *O*. These represent the drug diffusing to the receptor, and then binding or dissociating from the channel, respectively, as described previously [27]. The diffusion rate of flecainide was estimated at 5500 M^{-1} ms^{-1} [31].

2.2.   Simulation of I$_{Kr}$, I$_{to}$, or I$_{CaL}$ Blockade

To simulate the inhibitory effects of flecainide on I$_{Kr}$ I$_{to}$, or I$_{CaL}$ currents, we decreased the peak conductance, G$_X$ of each of these independent channels in a concentration dependent fashion using a concentration response relationship with a Hill coefficient of 1 ($n = 1$) as follow:

$$G_X = G_{X,max} \star \left(\frac{1}{1 + (Drug / IC_{50})^n} \right)$$

where G$_{X,max}$ is the nominal conductance value obtained from each ventricular myocyte model, and the IC$_{50}$ is the concentration of drug that produces a 50% inhibition of the targeted transmembrane current or intracellular organelle.

IC$_{50}$ values of drug to inhibit currents		
Currents	**IC$_{50}$**	**Reference**
I$_{RyR}$	20 μM	[27]
I$_{Kr}$	1.5 μM	[28]
I$_{to}$	15.2 μM	[29]
I$_{CaL}$	27.1 μM	[1]

2.3.   Fiber simulations

One-dimensional (1D) tissue was simulated as a fiber of 165 cells (1.65 cm) [32] with reflective boundary conditions. The diffusion coefficient D$_x$ was set to 0.00154 cm^2/ms to establish a conduction velocity of 60–73 cm/s in WT conditions [33]. Fibers were paced from 95 BPM to 150 BPM for 1500 beats. The last 100 beats of atrial or ventricular conducted action potentials of the middle cell and the major underlying ion currents were recorded for analysis.

2.4. QT intervals

The fiber (5.5 cm) was paced at varying cycle length from 554 to 943 ms for 200 beats in order to match the clinical data [34]. Pseudo ECGs were computed from the transmembrane potential V_m using the integral expression as in Gima and Rudy [35]. Heart rate corrected QT (QTc) was computed using Bazett's formula using the cubic root of RR interval [34].

$$QT_c = \frac{QT}{\sqrt{RR}}$$

Please see supplemental information for additional details about our previously published models used in this study. All source code to reproduce the simulated data here are freely available on the GitHub: https://github.com/ClancyLabUCD/Mechanisms-of-flecainide-induced-negative-inotropy-An-in-silico-study

3. Results

Flecainide is a classic "dirty drug" in that it binds to and affects multiple cardiac ionic targets [36]. We developed a computational model of the effects of flecainide to assess and integrate its effects on 5 targets in the heart including: I_{Na} (IC_{50} is dependent upon voltage, state and rate dependent [26]), I_{RyR} ($IC_{50} = 20$ μM [27]), I_{Kr} ($IC_{50} = 1.5$ μM [28]), I_{to} ($IC_{50} = 15.2$ μM [29]) and I_{caL} ($IC_{50} = 27.1$ μM [1]). We then used the model to simulate the rate-dependence and dose-dependence of the effects of flecainide on key cardiac parameters, including the Ca^{2+} handling as a proxy for the effects of flecainide on inotropy.

In Fig. 1, shows the comparison of experimental data in Panel A from the rat with the indicated doses (Fernandes et al., [8]) as follows: black dot (no drug), purple (0.18±0.03 μM), red (0.67±0.34 μM), gold (1.0±0.12 μM), and green (1.36±0.14 μM) and our simulations. In Panel B experimental data illustrating the effects of flecainide on canine hearts paced at 150±4 BPM is shown (plasma concentration at 5000 ng/mL, from van Middendorp et al., [13]). In Panel C, experimental data from the pig (4.8 μM, from Marum et al., [14]) is shown. Panels D, E and F show simulated data from the Grandi Bers human ventricular computational model indicating the relationship between the flecainide induced reduction in inotropy as a function of increased duration of the QRS complex. Panel D shows the dose dependent effect of flecainide (at 140 BPM with 2.5 (blue), 3.0 (green) and 4.8 (pink) μM) on peak intracellular Ca^{2+} transient and in Panel E these data are plotted as the integral of the Ca^{2+} transient (as a proxy for inotropy). The simulated QRS interval change as a function of flecainide reduction in peak I_{Na} is shown in Panel F. In Panel G the effects of flecainide from 0, 2.5 (left), 4 and 12 μM (right) on computed ventricular electrograms. Virtual myocytes were paced at 140 BPM. Note that conduction block developed at 4.8 μM flecainide in the simulation resulting in a dynamic timecourse shown during the last 7 beats of the simulation (pink symbols in Panels D, E and F). The simulations also revealed substantial rate-dependent effect of flecainide on QRS widening, as would be anticipated from the well-described use-dependent effects of flecainide in I_{Na} (Fig. 1G).

Fig. 2 shows the comparison of human clinical data from [34] and model predictions from simulated human tissues under drug free conditions and following low dose of flecainide (0.2 μM) and high dose of flecainide (2.0 μM) with varying pacing cycle lengths. The simulated ranges compared to clinically obtained data from humans are in good agreement, thereby providing an indication of the validity and predictive value of the computational results to recapitulate the effect of a flecainide on the human electrophysiology parameters including QRS interval, JT internal and QT interval.

We next undertook a more detailed investigation into the rate-dependent and dose-dependent effects on the relationship between predicted widening of the QRS interval and drug-induced negative inotropy. In Fig. 3, the predicted dose-dependent effects of flecainide are shown systematically from drug free (black), 0.5 (red), 1.0 (yellow), 1.5 (purple), 2.0 (green) to 2.5 (blue) μM. Rate-dependent (indicated heart rate from 95 to 145 BPM) widening of the QRS interval is shown in Panel A compared to peak I_{Na}. Panel B shows the widening of the QRS interval compared to the reduction in the peak intracellular Ca^{2+} transient and in Panel C as the reduction in the integral of the Ca^{2+} transient compared to widening of the QRS interval. Interestingly, the approximately linear correlation between the predicted increase in QRS duration and corresponding reduction in inotropy on Ca^{2+} transient did not significantly change with pacing frequency (Fig. 3D). Inotropy notably continued to decline at fast rates as QRS widening increased, indicated by the similar slopes of the relationships in panels B and C at faster pacing frequencies.

When the underlying ionic currents from a single virtual myocyte were examined in the tissue level simulations described above, we observed a profound slowing of the action potential upstroke (Fig. 4A), which is an expected consequence of I_{Na} block (Fig. 4B). In Fig. 4C-D, the mechanism of flecainide induced reduction in inotropy is revealed by the considerably reduced Ca^{2+} current (Panel C) and Ca^{2+} transient (panel D). The model predictions in a myocyte within a coupled tissue environment reveal the effect of flecainide to reduce the peak of L-type calcium current. This is due to slow conduction that allows the calcium channels to begin the inactivation process during slow depolarization [37].

As a result, the effect flecainide on a myocyte within coupled tissue (a syncytium) is not the same as what occurs in the single isolated myocyte. The predicted effect in a single simulated myocyte is shown in supplemental Fig. S1. In this case, the main effect of flecainide to reduce the upstroke velocity of the action potential results in a slowing of the depolarizing phase of the membrane potential, but the relative degree of slowing is much larger in coupled tissue. When sodium channels are blocked in the single isolated myocytes, the membrane voltage remains in a range that is favorable for calcium channel activation. In single myocytes shown in supplemental Fig. S1, the slowing of the AP upstroke results in an increase in calcium current at fast heart rates.

In order to further assess the mechanism underlying the negative inotropic effect of flecainide, we next conducted a series of "component dissection" simulations and ion monitoring to assess the primary effects of flecainide that lead to a reduction in the Ca^{2+} transient. The results are shown in Fig. 5. Our approach was to sequentially remove the effect of flecainide on individual ion current drug targets and then to assess the magnitude

of the effect on the changes in the Ca^{2+} transient. In doing so, we were able to reveal the relative contributions of flecainide effects on specific ion current targets to modification of the Ca^{2+} transient. In Fig. 5A from left to right, the effects of flecainide on all five simulated targets are shown for comparison on the peak I_{Na}, peak Ca^{2+} transient and the integral of the Ca^{2+} transient reduction.

When the effect of flecainide on the L-type Ca^{2+} current (I_{caL}) was eliminated (as in Fig. 5B), but the effect on the other four ion current targets remained, the negative inotropic effect of flecainide was reduced, but still persisted as indicated by peak I_{Na} reduction, the reduction in peak $[Ca^{2+}]$ and integral of the Ca^{2+} transient (from left to right). Interestingly, as shown in Fig. 5C, when the effect of flecainide on the L-type Ca^{2+} current (I_{caL}) and the ryanodine receptor (RyR) were both eliminated, but the effect on the other three ion current targets remained, flecainide still resulted in a reduction in the peak Ca^{2+} transient and the integral of the Ca^{2+} transient at the rapid heart rate shown (150 BPM).

A summary of the effects of flecainide during the elimination of selected flecainide targets is shown in the bar graphs in panel D, where the magnitude of the changes in the peak I_{Na}, the predicted peak Ca^{2+} transient and the integral of the Ca^{2+} transient are shown by the change in steepness of the relationships in the left, middle and right columns of panels A, B and C. For peak sodium, we computed the slope by calculating the change from the condition without drug to the point with the highest drug concentration to estimate the rate of change over the therapeutic plasma range. As expected, changes due to the reduction in peak I_{Na} is minimal as the effect of flecainide on I_{Na} is always included. These results suggest that the effect of flecainide to result in a negative inotropic outcome results in part from direct effects of the drug on proteins key for Ca^{2+} handling, consistent with earlier reports [38]. Both effects of flecainide on the L-type Ca^{2+} current (I_{caL}) and on the I_{RyR} contribute to negative inotropy.

We also investigated the effect of disruption to ion homeostasis under the conditions of rapid pacing in the presence of flecainide. As expected, shown in Fig. 6, simulations from ventricular myocytes indicate that the reduction in peak I_{Na} resulting from Na^+ channel block has the effect to reduce intracellular $[Na^+]$ by ~1 mM.

To determine whether the reduction in intracellular $[Na^+]$ contributes to flecainide-induced widening of simulated QRS and reduction in the Ca^{2+} transient, we paced the cells at 150 BPM within the therapeutic plasma range of 0.5 to 2.5 μM (red dots) with resulting reduced Ca^{2+} and compared this setting to the condition where intracellular sodium concentration was fixed at 9.7 mM (black asterisks). The results are shown in Fig. 7. There were minimal differences in the predicted effects of flecainide on 5 targets, (B) effects of flecainide on 4 targets and (C) effects of flecainide on 3 targets on the peak I_{Na}, peak Ca^{2+} transient and integral of the Ca^{2+} transient reduction from left to right. These simulations suggest that the reduction in intracellular Na^+ has a minimal effect to promote negative inotropy. Not surprisingly, the ~1 mM reduction in Na^+ most affects the amplitude of the Na^+ current and consequently the QRS interval, the effect is very small.

Here, we opted to utilize the Grandi-Bers computational model of the cardiac ventricular action potential because it has a well-characterized representation of $[Ca^{2+}]_i$ dynamics and homeostasis. However, to ensure that our findings were not dependent on the Grandi-Bers model, we also carried out simulations using the O'Hara-Rudy model, again focusing on assessing the relationship between flecainide-induced widening of simulated QRS and reduction in peak I_{Na}, peak Ca^{2+} transient, and integral of the Ca^{2+} transient at 150 BPM from drug free to 2.5 μM flecainide (Supplemental Fig. S2). The predictions generated by the O'Hara-Rudy model at drug doses greater than 1 μM were qualitatively similar to the predictions in the Grandi-Bers model.

It is important to note that while the modeling and simulation results in the prediction of the negative inotropy as assessed by a reduction in intracellular calcium in ventricular myocyte simulations, the effects predicted may constitute an underestimate. This is because additional hemodynamic effects are to be expected and likely exacerbated in disease states like atrial fibrillation [14,39-43].

We tested this in model simulations. We applied the flecainide effects on 5 ion current targets in simulated Grandi-Bers atrial cells I_{Na} ([26]), I_{RyR} ([27]), I_{Kr} (IC_{50} = 1.5 μM [28]), I_{to} (IC_{50} = 15.2 μM [29]) and I_{caL}(IC_{50} = 27.1 μM [1]). We tested the rate-dependence and dose-dependence of the effect of flecainide (0.5 and 1.0 μM) on the P wave duration and on the peak intracellular Ca^{2+} transient (Fig. 8A), and the integral of the Ca^{2+} transient (Fig. 8B), as a proxy for atrial inotropy. The flecainide effect on all targets results in an increase in the P wave duration a surrogate for the slowing of conduction in atrial tissue. However, when the effect of flecainide on the L-type Ca^{2+} current (I_{caL}) were eliminated, but the effect on the other four targets remained, the negative inotropic effect of flecainide persisted, but the AP upstroke was enhanced and the APD was prolonged with restoration of the Ca^{2+} current (Fig. 8C and D).

4. Discussion

In the study, developed and applied a human cardiac action potential modeling and simulation approach to reveal the mechanisms of negative inotropic affects that have been reported following application of flecainide and other similar sodium channel blockers. A reduction in the capacity of the heart to contract optimally after Na channel block has been described in a variety of species [8,38,44,45]. Understanding the ionic mechanisms of flecainide induced negative inotropy, may allow for the development of new or modified therapeutic approaches for diseases like atrial fibrillation that maintain the beneficial effects of flecainide as an antiarrhythmic drug target to normalize atrial dysrhythmia [46,14].

Indeed, conduction disturbances and mechanical dysfunction are aspects of safety pharmacology that have received relatively little attention. Most drug safety assessments associated with block of repolarization currents and consequent repolarization abnormalities. Even though more recent investigations into repolarization related safety pharmacology and its hallmark, the prolongation of the QT interval, have taken into account multi-channel block by drugs, there has not been a defined assay to consider the effects of depolarization abnormalities and mechanical dysfunction arising from ion channel block.

This important area of translational research is ripe for renewed investigation [6,37,10]. By assessing and revealing the fundamental ionic mechanisms associated with electrophysiological effects of flecainide and the resulting mechanical alterations, insights into promising development of new therapeutic interventions, or combinations of existing drugs used in appropriate doses may allow for minimization of unwanted side effects [47,48]. This may be critical for optimization of new methods for managing prevalent cardiac diseases like atrial fibrillation. Flecainide has been shown to be effective to convert atrial fibrillation to sinus rhythm. The most likely mechanisms for the antiarrhythmic effect is slowing of conduction and concomitant rate-dependent shortening of atrial refractoriness that sufficiently impact the fibrillatory wavelength to extinguish the arrhythmia [49].

A variety of mechanisms have been proposed as primary drivers of the negative inotropic effect of flecainide [38,50,51]. However there have been no experimental studies that systematically considered all plausible mechanisms and their individual contributions to negative inotropy. Moreover, these studies largely utilize drug concentrations that are not therapeutically relevant and so the application of findings to interpret clinical mechanisms is limited. Our findings bridge this gap by taking advantages of the strengths of computational modeling and simulation approaches that are well suited for such investigations. Modeling and simulation can also take into account the therapeutically relevant concentration of flecainide in order to establish the clinical relevance of our findings [52,53]. Moreover, modeling and simulation is uniquely suited to consider pharmacodynamic and kinetics, multi-channel effects and to assess the contributions of drug effects on individual targets to the overall drug efficacy [54-57].

The effects of flecainide on the L-type Ca^{2+} current [38,50] have been reported in many previous studies and this effect has been suggested as the likely mechanism for the negative inotropy promoted by flecainide. In the study by Kihara et al., the authors examined the differences in negative inotropy induced by flecainide and pilsicainide, both of which are classified as 1C anti-arrhythmic drugs. These two drugs block sodium channels similarly, but flecainide has more potent block of the L-type calcium channel. Indeed, the authors reported that with 10 μM application of flecainide, there was ~25% reduction in peak L-type Ca^{2+} current when measured in dog ventricular trabeculae [38]. They attributed the larger effect of flecainide to reduce inotropy as resulting from substantial block of the L-type Ca^{2+} current. The authors postulate that the reduced L-type Ca^{2+} current then reduced the calcium transient amplitude.

Other studies have reported flecainide to be less potent for inhibition of the L-type calcium current [1]. In the present study, we adopted a conservative approach and selected an $IC_{50} = 27.1$ μM [1] for flecainide inhibition of the L-type calcium current. Even the highest doses of clinically relevant flecainide are considerably lower (by an order of magnitude) and so any anticipated effect on the L-type calcium channel is likely to be very small. However, we did observe some rate dependent inhibitory effects presumably due to the build-up of flecainide in the L-type calcium channel and the related rate dependent reduction in the upstroke velocity of the action potential, due to use-dependent Na^+ channel block.

It is important to note that the effect of flecainide on the L-type calcium channel measured "in isolation" does not reflect what we observed in a more physiological setting. The effect of flecainide to reduce the upstroke velocity of the action potential results in a slowing of the depolarizing phase of the membrane potential (Fig. 4A). What this means practically is that when sodium channels are blocked the membrane voltage remains in a range that is favorable for calcium channel activation. Indeed, this effect in single simulated myocytes (shown in Supplemental Fig. S1) actually results in an increase in calcium current at fast heart rates. However, in simulated tissue under the same conditions assessed in the single simulated myocytes, the model simulations predicted the opposite. As shown in Fig. 4, the predictions in a model myocyte within a coupled tissue environment suggest a substantial effect of flecainide to reduce the peak of L-type calcium current. Part of the effect results from slow conduction that allows the calcium channels to begin the inactivation process during slow depolarization.

Other studies have suggested the importance of the Na/Ca exchanger in promoting the negative inotropic effect of flecainide [51]. Ito and coauthors reported that inhibition of Na^+ channels can result in changes to the Na^+/Ca^{2+} exchange current and ultimately leads to a decrease in the Ca^{2+} content in both the sarcoplasmic reticulum (SR) and Ca^{2+} entry through the exchanger. Fig. 6 shows the results of our simulations of these effects. Indeed, as suggested by Ito et al., we identified a substantial impact of Na^+ channel inhibition by flecainide to reduce intracellular $[Na^+]$ levels. We therefore tested the effect of preventing the reduction in intracellular $[Na^+]$ by clamping it to maintain drug free levels as shown in Fig. 7. The graphs in Fig. 7 indicate a small effect of the change in intracellular $[Na^+]$ that affects the magnitude of the Na^+/Ca^{2+} exchange current. Meme et al., [58], suggest under conditions of reduced intracellular $[Na^+]$, Ca^{2+} entry into the myocyte is likely to occur during diastole Na^+/Ca^{2+} exchange current rather than in systole via the L-type Ca^{2+} current. In our study, we primarily examined the effects of flecainide to reduce intracellular $[Na^+]$ during rapid pacing. In this setting the diastolic interval is short and does not allow time for loading via during diastole Na^+/Ca^{2+} exchange.

In summary, our human action potential and intracellular Ca^{2+} model simulations predict an interaction of multiple mechanisms that combine to result in the flecainide mediated reduction in cardiac contractile performance. In single isolated simulated myocytes, the reduction in I_{Na} acts to slow the upstroke velocity of the action potential and this can favor an increase in L-type Ca^{2+} current during the depolarizing phase. However, the modest increase in L-type Ca^{2+} current is offset by a reduction in outward NCX current that brings in notably less Ca^{2+} during the early phases of the action potential. Direct block of the RyR and L-type Ca^{2+} current by flecainide results in a reduction in both of these currents relative to the drug free condition. The net effect is a reduction in the peak and the integral of the Ca^{2+} transient which in turn results a reduction in inotropy. In the tissue level simulations, conduction of the depolarizing excitatory wave is hampered by flecainide block of I_{Na} that is exacerbated by electronic effects. In the tissue setting, simulated cells in the tissue exhibited a reduction in peak L-type Ca^{2+} current because the action potential upstroke was slow enough to allow channel inactivation. This effect is added to the reduction in outward NCX current and small amount of block of RyR by flecainide. Together, these effects lead to a substantial reduction in the predicted peak and the integral of the Ca^{2+} transient (Fig. 4).

We further applied a modeling and simulation approach and examined the relationship between flecainide application and the Ca^{2+} transient in computational atrial myocytes. Because of the different morphology of the atrial action potential, the dose and rate dependent reduction in the atrial Ca^{2+} transient following application of flecainide was more profound than in the ventricular simulations. The effect of the reduced capacity to carry out mechanical "squeeze" by the atria in the presence of flecainide would be expected to reduce ventricular filling and preload and consequently reduce dP/dt_{max} [59-61].

There are several limitations present in our study. Here, we tracked the peak of the Ca^{2+} transient (CaT) that has been linked to maximum contractile force [62], and the integral of the CaT as a more comprehensive indicator of the time course of the force of contraction over the entire cardiac cycle [63,64]. Clearly, the myofilament calcium sensitivity is a critical parameter that can affect the specific correlation of the relationship between CaT and contractile force. A limitation of our current model is that we do not explicitly account for the myofilament calcium sensitivity although it could be extended in a future state to include this and other features relevant to disease states [65]. Moreover, we do not explicitly represent stochastic phenomena such as calcium sparks that have shown to be inhibited by flecainide [66,67], although we and others have developed detailed models based on these data previously [27,68,69].

There are notable differenced in the results from the Grandi-Bers (GB) and O'Hara-Rudy (ORd) model predictions of the dose-dependence of flecainide effects on inotropy. Unlike the results predicted in Grandi-Bers, where we observed a dose-dependent reduction in inotropy, over the full range of simulated dose response in ORd, we observed a biphasic response. Whereas lower doses of flecainide caused an increase in the peak CaT in the ORd model, higher drug doses (1.5 μM and above) resulted in a decrease in contractility related parameters as shown in Supplemental Fig. S2. Indeed, the model described by Tomek et al. in the ToR-ORd model was developed in part to address the observed increase in Ca^{2+} in response to Na^+ channel block [70].

In addition to the differences in the representation of the Na^+ current in earlier models, the GB and ORd models have different approaches to of Ca^{2+} handling and incorporate different local subspaces. The GB model predicts separate Na^+ and Ca^{2+} concentrations in the junctional cleft, sub-sarcolemma (SL) and cytosol as well as accounting for the concentration of Ca^{2+} in the sarcoplasmic reticulum (SR). However, the ORd model included two compartments representing separate cytosol and junctional cleft concentrations for Na^+ and Ca^{2+}, along with junctional and network SR Ca^{2+} concentrations. I_{CaL} is also distributed differently in the GB model, with 10% of channels in the SL and 90% in the junctional cleft (in close proximity to the T-tubules and RyR Ca^{2+} release channels). In the ORd model, the I_{CaL} was located only in the junctional cleft, and I_{NaCa} was distributed as 20% in the junctional cleft and 80% in cytosol. In addition, in the GB model, the I_{CaL} peak was broader than in the ORd model, and the decay rate of CaT was slower in the Ord model compared to GB model.

The ToR-ORd model [70] includes additional modifications and represents an updated version that includes I_{CaL}, I_{Na}, I_{kr} (replaced by a Markov model), and I_{k1}. I_{CaL} was

particularly revised in terms of its driving force, activation curve, and location – 20% of I_{CaL} was placed in cytosolic space. The calcium-sensitive chloride current and background chloride current from GB model were also added into the ToR-ORd model. Other changes in ionic conductance parameters included I_{to}, I_{kKs}, I_{NaCa}, I_{NaK}, I_{Kb}, I_{Nab}, I_{Cab}, I_{pCa}, J_{rel}, and J_{up}.

We recognize that all models have strengths and weaknesses and that models continue to undergo continuous development. Indeed, a potential perceived weakness of the model used to represent the interaction of flecainide with the Na^+ channel in this study is complex. However, despite having recently constructed a reduced simplified Hodgkin-Huxley model of lidocaine interaction with the Na current where we show that we can reproduce the basic properties of lidocaine block (arXiv:2102.02342), we were not able to similarly develop a reduced model of the Na^+ channel interaction with flecainide. We were unable to reduce the model and still reproduce the slow complex time course of recovery from block and the voltage dependence of use-dependent block, which we have shown in earlier studies is the signature of flecainide interaction with the Na^+ channel [26,27]. In other words, we know that a simple reduction of the conductance of the Na^+ channel will not yield realistic block of the Na^+ current. In the case of flecainide, the rapid gating kinetics of the Na^+ channel and the slow drug kinetics of flecainide create the complex dynamics of flecainide block of Na^+ current.

Future studies could consider the impact of additional disease states, which may further complicate the interpretation of safety of Na^+ channel blockers as effective antiarrhythmic agents [9,14,39-43]. Indeed, the study by Gao et al. revealed compromised contractility in heart failure, but also identified an altered response to pharmacological manipulation by a variety of agents, including flecainide. In de Antonio et al. the importance of rate-dependence of disease can allow for selective atrial versus ventricular drug efficacy, a promising approach in atrial fibrillation [41]. A limitation of our results presented in this study is that they do not include predictions in the diseased heart. Future studies will be carried out to allow for study of disease states.

Supplementary Material

Refer to Web version on PubMed Central for supplementary material.

Support

References

[1]. Kramer J, Obejero-Paz CA, Myatt G, Kuryshev YA, Bruening-Wright A, Verducci JS, et al. , MICE models: superior to the HERG model in predicting Torsade de Pointes, Sci. Rep 3 (2013) 2100. Epub 2013/07/03, 10.1038/srep02100 (PubMed PMID: 23812503; PubMed Central PMCID: PMCPMC3696896). [PubMed: 23812503]

[2]. Li Z, Mirams GR, Yoshinaga T, Ridder BJ, Han X, Chen JE, et al. , General principles for the validation of proarrhythmia risk prediction models: an extension of the CiPA in silico strategy,

Clin. Pharmacol. Ther 107 (1) (2020) 102–111. Epub 2019/11/12, 10.1002/cpt.1647 (PubMed PMID: 31709525; PubMed Central PMCID: PMCPMC6977398). [PubMed: 31709525]

[3]. Waldo AL, Camm AJ, de Ruyter H, Freidman PL, MacNeil DJ, Pitt B, et al. , Survival with oral d-sotalol in patients with left ventricular dysfunction after myocardial infarction: rationale, design, and methods (the SWORD trial), Am. J. Cardiol 75 (15) (1995) 1023–1027. Epub 1995/05/15, 10.1016/s0002-9149(99)80717-6 (PubMed PMID: 7747682). [PubMed: 7747682]

[4]. Rampe D, Brown AM, A history of the role of the hERG channel in cardiac risk assessment, J. Pharmacol. Toxicol. Methods 68 (1) (2013) 13–22. Epub 2013/03/30, 10.1016/j.vascn.2013.03.005 (PubMed PMID: 23538024).

[5]. Ridder BJ, Leishman DJ, Bridgland-Taylor M, Samieegohar M, Han X, Wu WW, et al. , A systematic strategy for estimating hERG block potency and its implications in a new cardiac safety paradigm, Toxicol. Appl. Pharmacol 394 (2020) 114961. Epub 2020/03/27, 10.1016/j.taap.2020.114961 (PubMed PMID: 32209365; PubMed Central PMCID: PMCPMC7166077). [PubMed: 32209365]

[6]. Venkatasubramanian R, Collins TA, Lesko LJ, Mettetal JT, Trame MN, Semi-mechanistic modelling platform to assess cardiac contractility and haemodynamics in preclinical cardiovascular safety profiling of new molecular entities, Br. J. Pharmacol 177 (15) (2020) 3568–3590. Epub 2020/04/27, 10.1111/bph.15079 (PubMed PMID: 32335903; PubMed Central PMCID: PMCPMC7348097). [PubMed: 32335903]

[7]. Erdemli G, Kim AM, Ju H, Springer C, Penland RC, Hoffmann PK, Cardiac safety implications of hNav1.5 Blockade and a framework for pre-clinical evaluation, Front. Pharmacol 3 (2012) 6. Epub 2012/02/04, 10.3389/fphar.2012.00006 (PubMed PMID: 22303294; PubMed Central PMCID: PMCPMC3266668). [PubMed: 22303294]

[8]. Fernandes S, Hoyer K, Liu G, Wang WQ, Dhalla AK, Belardinelli L, et al. , Selective inhibition of the late sodium current has no adverse effect on electrophysiological or contractile function of the normal heart, J. Cardiovasc. Pharmacol 63 (6) (2014) 512–519. Epub 2014/01/11. [PubMed: 24406487]

[9]. Gao B, Qu Y, Sutherland W, Chui RW, Hoagland K, Vargas HM, Decreased contractility and altered responses to inotropic agents in myocytes from tachypacing-induced heart failure canines, J. Pharmacol. Toxicol. Methods 93 (2018) 98–107. Epub 2018/06/17. [PubMed: 29908289]

[10]. Butler L, Cros C, Oldman KL, Harmer AR, Pointon A, Pollard CE, et al. , Enhanced characterization of contractility in cardiomyocytes during early drug safety assessment, Toxicol. Sci 145 (2) (2015) 396–406. Epub 2015/03/31, 10.1093/toxsci/kfv062 (PubMed PMID: 25820236). [PubMed: 25820236]

[11]. Caron J, Libersa C, Adverse effects of class I antiarrhythmic drugs, Drug Saf. 17 (1) (1997) 8–36. Epub 1997/07/01. [PubMed: 9258628]

[12]. Josephson MA, Ikeda N, Singh BN, Effects of flecainide on ventricular function: clinical and experimental correlations, Am. J. Cardiol 53 (5) (1984) 95B–100B. Epub 1984/02/27, 10.1016/0002-9149(84)90510-1 (PubMed PMID: 6695822).

[13]. van Middendorp LB, Strik M, Houthuizen P, Kuiper M, Maessen JG, Auricchio A, et al. , Electrophysiological and haemodynamic effects of vernakalant and flecainide in dyssynchronous canine hearts, Europace 16 (8) (2014) 1249–1256. Epub 2014/02/01, 10.1093/europace/eut429 (PubMed PMID: 24481779). [PubMed: 24481779]

[14]. Marum AA, Silva BA, Bortolotto AL, Silva AC, de Antonio VZ, Belardinelli L, et al. , Optimizing flecainide plasma concentration profile for atrial fibrillation conversion while minimizing adverse ventricular effects by rapid, low-dose intratracheal or intravenous administration, Int. J. Cardiol 274 (2019) 170–174. Epub 2018/09/16, 10.1016/j.ijcard.2018.09.029 (PubMed PMID: 30217428). [PubMed: 30217428]

[15]. Block PJ, Winkle RA, Hemodynamic effects of antiarrhythmic drugs, Am. J. Cardiol 52 (6) (1983) 14C–23C. Epub 1983/09/22, 10.1016/0002-9149(83)90627-6 (PubMed PMID: 6414278). [PubMed: 6602539]

[16]. Schlepper M, Cardiodepressive effects of antiarrhythmic drugs, Eur. Heart J 10 (Suppl E) (1989) 73–80. Epub 1989/09/01, 10.1093/eurheartj/10.suppl_e.73 (PubMed PMID: 2553412).

[17]. Woosley RL, Echt DS, Roden DM, Effects of congestive heart failure on the pharmacokinetics and pharmacodynamics of antiarrhythmic agents, Am. J. Cardiol 57 (3) (1986) 25B–33B. Epub 1986/01/31, 10.1016/0002-9149(86)90995-1 (PubMed PMID: 3080860).

[18]. Lynch JJ Jr., Regan CP, Beatch GN, Gleim GW, Morabito CJ, Comparison of the intrinsic vasorelaxant and inotropic effects of the antiarrhythmic agents vernakalant and flecainide in human isolated vascular and cardiac tissues, J. Cardiovasc. Pharmacol 61 (3) (2013) 226–232. Epub 2012/11/29. [PubMed: 23188129]

[19]. Sugiyama A, Takehana S, Kimura R, Hashimoto K, Negative chronotropic and inotropic effects of class I antiarrhythmic drugs assessed in isolated canine blood-perfused sinoatrial node and papillary muscle preparations, Heart Vessel. 14 (2) (1999) 96–103. Epub 2000/01/29, 10.1007/BF02481749 (PubMed PMID: 10651186).

[20]. Echt DS, Liebson PR, Mitchell LB, Peters RW, Obias-Manno D, Barker AH, et al. , Mortality and morbidity in patients receiving encainide, flecainide, or placebo. The cardiac arrhythmia suppression trial, N. Engl. J. Med 324 (12) (1991) 781–788. Epub 1991/03/21, 10.1056/NEJM199103213241201 (PubMed PMID: 1900101). [PubMed: 1900101]

[21]. Grandi E, Pasqualini FS, Bers DM, A novel computational model of the human ventricular action potential and Ca transient, J. Mol. Cell Cardiol 48 (1) (2010) 112–121. Epub 2009/10/20, 10.1016/j.yjmcc.2009.09.019 (PubMed PMID: 19835882; PubMed Central PMCID: PMCPMC2813400). [PubMed: 19835882]

[22]. Breindahl T, Therapeutic drug monitoring of flecainide in serum using high-performance liquid chromatography and electrospray mass spectrometry, J. Chromatogr. B Biomed. Sci. Appl 746 (2) (2000) 249–254. Epub 2000/11/15, 10.1016/s0378-4347(00)00343-1 (PubMed PMID: 11076078). [PubMed: 11076078]

[23]. Conard GJ, Ober RE, Metabolism of flecainide, Am. J. Cardiol 53 (5) (1984) 41B–51B. Epub 1984/02/27, 10.1016/0002-9149(84)90501-0 (PubMed PMID: 6364769).

[24]. Grandi E, Pandit SV, Voigt N, Workman AJ, Dobrev D, Jalife J, et al. , Human atrial action potential and Ca2+ model: sinus rhythm and chronic atrial fibrillation, Circ. Res 109 (9) (2011) 1055–1066. Epub 2011/09/17, 10.1161/CIRCRESAHA.111.253955 (PubMed PMID: 21921263; PubMed Central PMCID: PMC3208665). [PubMed: 21921263]

[25]. O'Hara T, Virag L, Varro A, Rudy Y, Simulation of the undiseased human cardiac ventricular action potential: model formulation and experimental validation, PLoS Comput. Biol 7 (5) (2011), e1002061. Epub 2011/06/04, 10.1371/journal.pcbi.1002061 (PubMed PMID: 21637795; PubMed Central PMCID: PMCPMC3102752). [PubMed: 21637795]

[26]. Moreno JD, Zhu ZI, Yang PC, Bankston JR, Jeng MT, Kang C, et al. , A computational model to predict the effects of class I anti-arrhythmic drugs on ventricular rhythms, Sci. Transl. Med 3 (98) (2011), 98ra83. Epub 2011/09/03. doi: 3/98/98ra83 [pii], 10.1126/scitranslmed.3002588 (PubMed PMID: 21885405).

[27]. Yang PC, Moreno JD, Miyake CY, Vaughn-Behrens SB, Jeng MT, Grandi E, et al. , In silico prediction of drug therapy in catecholaminergic polymorphic ventricular tachycardia, J. Physiol 594 (3) (2016) 567–593. Epub 2015/10/31, 10.1113/JP271282 (PubMed PMID: 26515697; PubMed Central PMCID: PMCPMC4784170). [PubMed: 26515697]

[28]. Belardinelli L, Liu G, Smith-Maxwell C, Wang WQ, El-Bizri N, Hirakawa R, et al. , A novel, potent, and selective inhibitor of cardiac late sodium current suppresses experimental arrhythmias, J. Pharmacol. Exp. Ther 344 (1) (2013) 23–32. Epub 2012/09/27, 10.1124/jpet.112.198887 (PubMed PMID: 23010360). [PubMed: 23010360]

[29]. Slawsky MT, Castle NA, K+ channel blocking actions of flecainide compared with those of propafenone and quinidine in adult rat ventricular myocytes, J. Pharmacol. Exp. Ther 269 (1) (1994) 66–74. Epub 1994/04/01, 8169853. [PubMed: 8169853]

[30]. Shannon TR, Wang F, Puglisi J, Weber C, Bers DM, A mathematical treatment of integrated Ca dynamics within the ventricular myocyte, Biophys. J 87 (5) (2004) 3351–3371. Epub 2004/09/07, 10.1529/biophysj.104.047449 (PubMed PMID: 15347581; PubMed Central PMCID: PMC1304803). [PubMed: 15347581]

[31]. Zhu Y, Kyle JW, Lee PJ, Flecainide sensitivity of a Na channel long QT mutation shows an open-channel blocking mechanism for use-dependent block, Am. J. Physiol. Heart Circ.

Physiol 291 (1) (2006) H29–H37. Epub 2006/02/28, 10.1152/ajpheart.01317.2005 (PubMed PMID: 16501012). [PubMed: 16501012]

[32]. Glukhov AV, Fedorov VV, Lou Q, Ravikumar VK, Kalish PW, Schuessler RB, et al. , Transmural dispersion of repolarization in failing and nonfailing human ventricle, Circ. Res 106 (5) (2010) 981–991. Epub 2010/01/23. doi: CIRCRESAHA. 109.204891 [pii], 10.1161/ CIRCRESAHA.109.204891 (PubMed PMID: 20093630). [PubMed: 20093630]

[33]. Brugada J, Boersma L, Kirchhof C, Allessie M, Anisotropy and reentrant ventricular tachycardia: experimental model in the isolated rabbit heart, Rev. Espan. Cardiol 43 (8) (1990) 558–568 (Epub 1990/10/01. PubMed PMID: 2099516).

[34]. Hellestrand KJ, Bexton RS, Nathan AW, Spurrell RA, Camm AJ, Acute electrophysiological effects of flecainide acetate on cardiac conduction and refractoriness in man, Br. Heart J 48 (2) (1982) 140–148. Epub 1982/08/01, 10.1136/hrt.48.2.140 (PubMed PMID: 7093083; PubMed Central PMCID: PMCPMC481218). [PubMed: 7093083]

[35]. Gima K, Rudy Y, Ionic current basis of electrocardiographic waveforms: a model study, Circ. Res 90 (8) (2002) 889–896 (Epub 2002/05/04. PubMed PMID: 11988490). [PubMed: 11988490]

[36]. Mehra D, Imtiaz MS, van Helden DF, Knollmann BC, Laver DR, Multiple modes of ryanodine receptor 2 inhibition by flecainide, Mol. Pharmacol 86 (6) (2014) 696–706. Epub 2014/10/03, 10.1124/mol.114.094623 (PubMed PMID: 25274603; PubMed Central PMCID: PMCPMC4244595). [PubMed: 25274603]

[37]. Fletcher S, Maddock H, James RS, Wallis R, Gharanei M, The cardiac work-loop technique: an in vitro model for identifying and profiling drug-induced changes in inotropy using rat papillary muscles, Sci Rep 10 (1) (2020), 5258. Epub 2020/03/27, 10.1038/s41598-020-58935-2 (PubMed PMID: 32210283; PubMed Central PMCID: PMCPMC7093439). [PubMed: 32210283]

[38]. Kihara Y, Inoko M, Hatakeyama N, Momose Y, Sasayama S, Mechanisms of negative inotropic effects of class Ic antiarrhythmic agents: comparative study of the effects of flecainide and pilsicainide on intracellular calcium handling in dog ventricular myocardium, J. Cardiovasc. Pharmacol 27 (1) (1996) 42–51. Epub 1996/01/01. [PubMed: 8656657]

[39]. Verrier RL, Belardinelli L, Pulmonary delivery of antiarrhythmic drugs for rapid conversion of new-onset atrial fibrillation, J. Cardiovasc. Pharmacol 75 (4) (2020) 276–283. Epub 2020/02/08, 10.1097/FJC.0000000000000804 (PubMed PMID: 32032206; PubMed Central PMCID: PMCPMC7161718). [PubMed: 32032206]

[40]. Tessarolo Silva F, Pedreira GC, Medeiros SA, Bortolotto AL, Araujo Silva B, Hurrey M, et al. , Multimodal mechanisms and enhanced efficiency of atrial fibrillation cardioversion by pulmonary delivery of a novel flecainide formulation, J. Cardiovasc. Electrophysiol 31 (1) (2020) 205–213. Epub 2019/11/22, 10.1111/jce.14289 (PubMed PMID: 31749267). [PubMed: 31749267]

[41]. de Antonio VZ, Silva AC, Stocco FG, Silva BA, Marum AA, Bortolotto AL, et al. , Pulmonary delivery of flecainide causes a rate-dependent predominant effect on atrial compared with ventricular depolarization duration revealed by intracardiac recordings in an intact porcine model, J. Cardiovasc. Electrophysiol 29 (11) (2018) 1563–1569. Epub 2018/08/15. [PubMed: 30106207]

[42]. Verrier RL, Bortolotto AL, Silva BA, Marum AA, Stocco FG, Evaristo E, et al. , Accelerated conversion of atrial fibrillation to normal sinus rhythm by pulmonary delivery of flecainide acetate in a porcine model, Heart Rhythm. 15 (12) (2018) 1882–1888. Epub 2018/07/01, 10.1016/j.hrthm.2018.06.036 (PubMed PMID: 29958990). [PubMed: 29958990]

[43]. Stocco FG, Evaristo E, Silva AC, de Antonio VZ, Pfeiffer J, Rangachari N, et al. , Comparative pharmacokinetic and electrocardiographic effects of intratracheal and intravenous administration of flecainide in anesthetized pigs, J. Cardiovasc. Pharmacol 72 (3) (2018) 129–135. Epub 2018/06/21, 10.1097/FJC.0000000000000605 (PubMed PMID: 29923887). [PubMed: 29923887]

[44]. Holtzman JL, Finley D, Mottonen L, Berry DA, Ekholm BP, Kvam DC, et al. , The pharmacodynamic and pharmacokinetic interaction between single doses of flecainide acetate and verapamil: effects on cardiac function and drug clearance, Clin. Pharmacol. Ther 46 (1) (1989) 26–32. Epub 1989/07/01, 10.1038/clpt.1989.102 (PubMed PMID: 2501057). [PubMed: 2501057]

[45]. Twidale N, Roberts-Thomson P, McRitchie RJ, Chalmers JP, Comparative haemodynamic effects of verapamil, flecainide, amiodarone and sotalol in the conscious rabbit, Clin. Exp. Pharmacol.

Physiol 21 (3) (1994) 179–188. Epub 1994/03/01, 10.1111/j.1440-1681.1994.tb02493.x (PubMed PMID: 8076419). [PubMed: 8076419]

[46]. Naccarelli GV, Wolbrette DL, Khan M, Bhatta L, Hynes J, Samii S, et al. , Old and new antiarrhythmic drugs for converting and maintaining sinus rhythm in atrial fibrillation: comparative efficacy and results of trials, Am. J. Cardiol 91 (6A) (2003) 15D–26D. Epub 2003/04/03, 10.1016/s0002-9149(02)03375-1 (PubMed PMID: 12670638).

[47]. Gjermeni E, Bollmann A, Hindricks G, Mussigbrodt A, Flecainide-associated cardiogenic shock in a patient with atrial fibrillation, Case Rep. Cardiol 2019 (2019), 4820652. Epub 2019/12/13, 10.1155/2019/4820652 (PubMed PMID: 31827935; PubMed Central PMCID: PMCPMC6885768). [PubMed: 31827935]

[48]. Santinelli V, Arnese M, Oppo I, Matarazzi C, Maione S, Palma M, et al. , Effects of flecainide and propafenone on systolic performance in subjects with normal cardiac function, Chest 103 (4) (1993) 1068–1073. Epub 1993/04/01, 10.1378/chest.103.4.1068 (PubMed PMID: 8131440). [PubMed: 8131440]

[49]. Andrikopoulos GK, Pastromas S, Tzeis S, Flecainide: current status and perspectives in arrhythmia management, World J. Cardiol 7 (2) (2015) 76–85. Epub 2015/02/27, 10.4330/wjc.v7.i2.76 (PubMed PMID: 25717355; PubMed Central PMCID: PMCPMC4325304). [PubMed: 25717355]

[50]. Scamps F, Undrovinas A, Vassort G, Inhibition of ICa in single frog cardiac cells by quinidine, flecainide, ethmozin, and ethacizin, Am. J. Phys 256 (3 Pt 1) (1989) C549–C559. Epub 1989/03/01, 10.1152/ajpcell.1989.256.3.C549 (PubMed PMID: 2538064).

[51]. Ito K, Nagafuchi K, Taga A, Yorikane R, Koike H, Possible involvement of altered Na+ −Ca2+ exchange in negative inotropic effects of class I antiarrhythmic drugs on rabbit and rat ventricles, J. Cardiovasc. Pharmacol 27 (3) (1996) 355–361. Epub 1996/03/01, 10.1097/00005344-199603000-00007 (PubMed PMID: 8907796). [PubMed: 8907796]

[52]. Yang PC, Purawat S, Ieong PU, Jeng MT, DeMarco KR, Vorobyov I, et al. , A demonstration of modularity, reuse, reproducibility, portability and scalability for modeling and simulation of cardiac electrophysiology using Kepler Workflows, PLoS Comput. Biol 15 (3) (2019), e1006856. Epub 2019/03/09, 10.1371/journal.pcbi.1006856 (PubMed PMID: 30849072; PubMed Central PMCID: PMCPMC6426265). [PubMed: 30849072]

[53]. Clancy CE, An G, Cannon WR, Liu Y, May EE, Ortoleva P, et al. , Multiscale modeling in the clinic: drug design and development, Ann. Biomed. Eng 44 (9) (2016) 2591–2610. Epub 2016/02/18, 10.1007/s10439-016-1563-0 (PubMed PMID: 26885640; PubMed Central PMCID: PMCPMC4983472). [PubMed: 26885640]

[54]. Doki K, Kuga K, Aonuma K, Ieda M, Homma M, Utilizing physiologically based pharmacokinetic modeling to predict theoretically conceivable extreme elevation of serum flecainide concentration in an anuric hemodialysis patient with cirrhosis, Eur. J. Clin. Pharmacol 76 (6) (2020) 821–831. Epub 2020/04/07. [PubMed: 32249350]

[55]. Bai J, Lo A, Gladding PA, Stiles MK, Fedorov VV, Zhao J, In silico investigation of the mechanisms underlying atrial fibrillation due to impaired Pitx2, PLoS Comput Biol. 16 (2) (2020), e1007678. Epub 2020/02/26, 10.1371/journal.pcbi.1007678 (PubMed PMID: 32097431; PubMed Central PMCID: PMCPMC7059955). [PubMed: 32097431]

[56]. Cars T, Lindhagen L, Malmstrom RE, Neovius M, Schwieler J, Wettermark B, et al. , Effectiveness of drugs in routine care: a model for sequential monitoring of new medicines using dronedarone as example, Clin. Pharmacol. Ther 103 (3) (2018) 493–501. Epub 2017/06/01, 10.1002/cpt.751 (PubMed PMID: 28560722). [PubMed: 28560722]

[57]. Veeraraghavan R, Lin J, Hoeker GS, Keener JP, Gourdie RG, Poelzing S, Sodium channels in the Cx43 gap junction perinexus may constitute a cardiac ephapse: an experimental and modeling study, Pflugers Arch. 467 (10) (2015) 2093–2105. Epub 2015/01/13, 10.1007/s00424-014-1675-z (PubMed PMID: 25578859; PubMed Central PMCID: PMCPMC4500747). [PubMed: 25578859]

[58]. Meme W, O'Neill S, Eisner D, Low sodium inotropy is accompanied by diastolic Ca2+ gain and systolic loss in isolated guinea-pig ventricular myocytes, J. Physiol 530 (Pt 3) (2001) 487–495. Epub 2001/02/07, 10.1111/j.1469-7793.2001.0487k.x (PubMed PMID: 11158278; PubMed Central PMCID: PMCPMC2278415). [PubMed: 11158278]

[59]. Quinones MA, Gaasch WH, Alexander JK, Influence of acute changes in preload, afterload, contractile state and heart rate on ejection and isovolumic indices of myocardial contractility in man, Circulation 53 (2) (1976) 293–302. Epub 1976/02/01, 10.1161/01.cir.53.2.293 (PubMed PMID: 1245037). [PubMed: 1245037]

[60]. Konishi T, Nakamura Y, Kato I, Kawai C, Dependence of peak dP/dt and mean ejection rate on load and effect of inotropic agents on the relationship between peak dP/dt and left ventricular developed pressure—assessed in the isolated working rat heart and cardiac muscles, Int. J. Cardiol 35 (3) (1992) 333–341. Epub 1992/06/01, 10.1016/0167-5273(92)90231-q (PubMed PMID: 1612796). [PubMed: 1612796]

[61]. Blaudszun G, Licker MJ, Morel DR, Preload-adjusted left ventricular dP/dtmax: a sensitive, continuous, load-independent contractility index, Exp. Physiol 98 (10) (2013) 1446–1456. Epub 2013/06/25, 10.1113/expphysiol.2013.073833 (PubMed PMID: 23794678). [PubMed: 23794678]

[62]. Gao WD, Atar D, Backx PH, Marban E, Relationship between intracellular calcium and contractile force in stunned myocardium. Direct evidence for decreased myofilament Ca2+ responsiveness and altered diastolic function in intact ventricular muscle, Circ. Res 76 (6) (1995) 1036–1048. Epub 1995/06/01, 10.1161/01.res.76.6.1036 (PubMed PMID: 7758158). [PubMed: 7758158]

[63]. Eisner DA, Caldwell JL, Kistamas K, Trafford AW, Calcium and excitation-contraction coupling in the heart, Circ. Res 121 (2) (2017) 181–195. Epub 2017/07/08, 10.1161/CIRCRESAHA.117.310230 (PubMed PMID: 28684623; PubMed Central PMCID: PMCPMC5497788). [PubMed: 28684623]

[64]. Saleem U, Mannhardt I, Braren I, Denning C, Eschenhagen T, Hansen A, Force and calcium transients analysis in human engineered heart tissues reveals positive force-frequency relation at physiological frequency, Stem Cell Rep. 14 (2) (2020) 312–324. Epub 2020/01/21, 10.1016/j.stemcr.2019.12.011 (PubMed PMID: 31956082; PubMed Central PMCID: PMCPMC7013237).

[65]. Chung JH, Biesiadecki BJ, Ziolo MT, Davis JP, Janssen PM, Myofilament calcium sensitivity: role in regulation of in vivo cardiac contraction and relaxation, Front Physiol. 7 (2016) 562. Epub 2016/12/27, 10.3389/fphys.2016.00562 (PubMed PMID: 28018228; PubMed Central PMCID: PMCPMC5159616). [PubMed: 28018228]

[66]. Sikkel MB, Collins TP, Rowlands C, Shah M, O'Gara P, Williams AJ, et al. , Flecainide reduces Ca(2+) spark and wave frequency via inhibition of the sarcolemmal sodium current, Cardiovasc Res. 98 (2) (2013) 286–296. Epub 2013/01/22, 10.1093/cvr/cvt012 (PubMed PMID: 23334259; PubMed Central PMCID: PMCPMC3714924). [PubMed: 23334259]

[67]. Hilliard FA, Steele DS, Laver D, Yang Z, Le Marchand SJ, Chopra N, et al. , Flecainide inhibits arrhythmogenic Ca2+ waves by open state block of ryanodine receptor Ca2+ release channels and reduction of Ca2+ spark mass, J. Mol. Cell Cardiol 48 (2) (2010) 293–301. Epub 2009/10/20, 10.1016/j.yjmcc.2009.10.005 (PubMed PMID: 19835880; PubMed Central PMCID: PMCPMC2813417). [PubMed: 19835880]

[68]. Song Z, Karma A, Weiss JN, Qu Z, Long-lasting sparks: multi-metastability and release competition in the calcium release unit network, PLoS Comput Biol. 12 (1) (2016), e1004671. Epub 2016/01/06, 10.1371/journal.pcbi.1004671 (PubMed PMID: 26730593; PubMed Central PMCID: PMCPMC4701461). [PubMed: 26730593]

[69]. Johnson DM, Heijman J, Bode EF, Greensmith DJ, van der Linde H, Abi-Gerges N, et al. , Diastolic spontaneous calcium release from the sarcoplasmic reticulum increases beat-to-beat variability of repolarization in canine ventricular myocytes after beta-adrenergic stimulation, Circ. Res 112 (2) (2013) 246–256. Epub 2012/11/15, 10.1161/CIRCRESAHA.112.275735 (PubMed PMID: 23149594). [PubMed: 23149594]

[70]. Tomek J, Bueno-Orovio A, Passini E, Zhou X, Minchole A, Britton O, et al. , Development, calibration, and validation of a novel human ventricular myocyte model in health, disease, and drug block, Elife (2019) 8. Epub 2019/12/24, 10.7554/eLife.48890 (PubMed PMID: 31868580; PubMed Central PMCID: PMCPMC6970534).
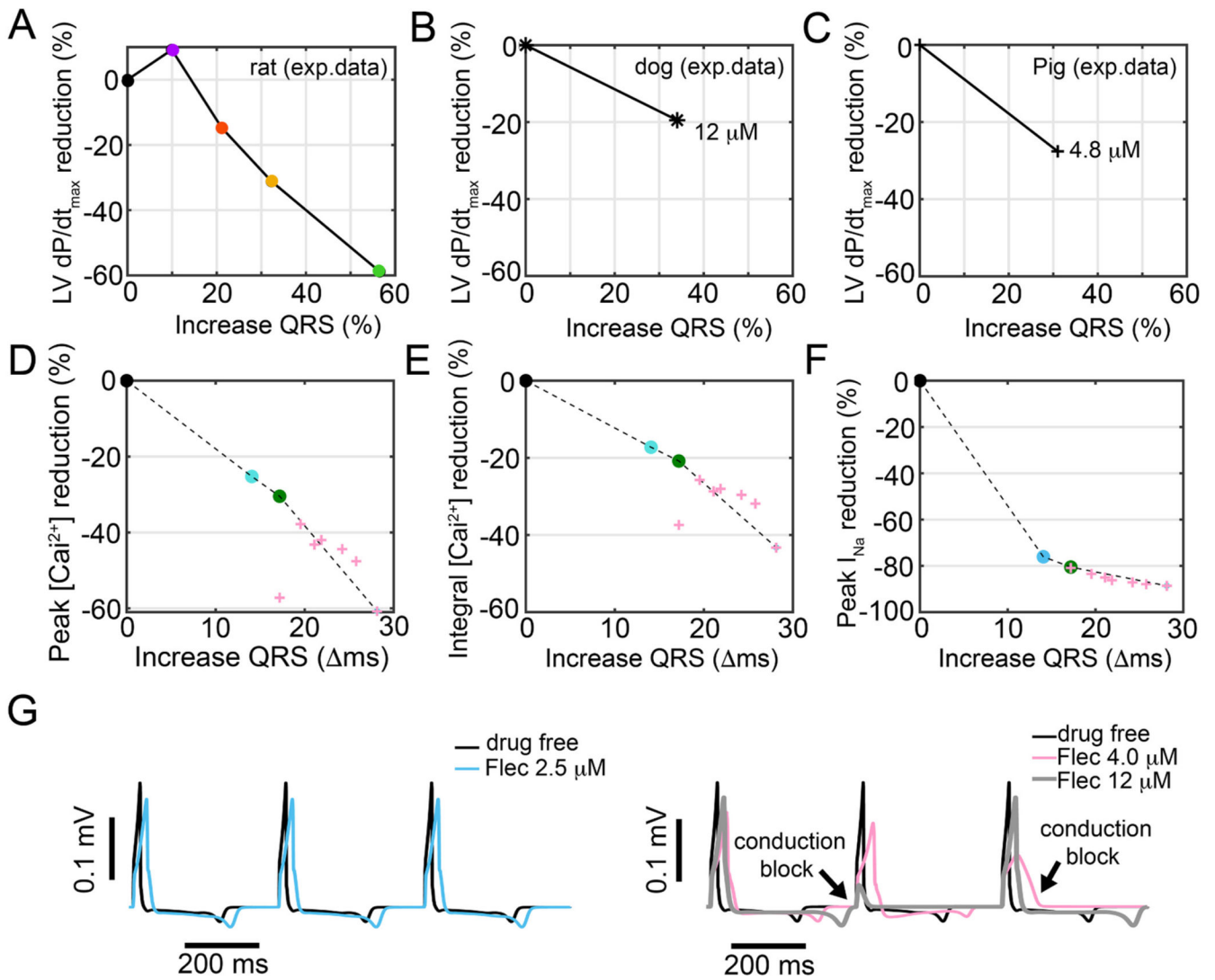
Fig. 1.
Correlation between flecainide-induced widening of a surrogate measure for the QRS complex and reduction in LV dP/dt$_{max}$ in a (A) Langendorff rat heart with the indicated doses (Fernandes et al., [8]). (a: 0.18±0.03 μM, b: 0.67±0.34 μM, c: 1.0±0.12 μM, and d: 1.36±0.14 μM) (B) Canine hearts paced at 150±4 BPM and reached a plasma concentration at 5000 ng/mL (van Middendorp et al., [13]). (C) Pig hearts paced at 140 BPM with IT administration of flecainide (1.5 mg/kg, bolus) and reached C$_{max}$ at 2000 ng/mL (approximately 4.8 μM - pink). Predicted effects in human ventricular computational tissue of flecainide on the relationship between the widening of QRS complex and (D) the peak intracellular Ca^{2+} transient, and (E) the integral of the Ca^{2+} transient, and (F) the peak I$_{Na}$ at 140 BPM with 2.5 (blue), 3.0 (green) and 4.8 (pink) μM. (G) Effects of flecainide of 0, 2.5 (left), 4 and 12 μM (right) on computed ventricular electrograms. Myocytes were paced at 140 BPM. Conduction block was observed when flecainide 4.0 μM.
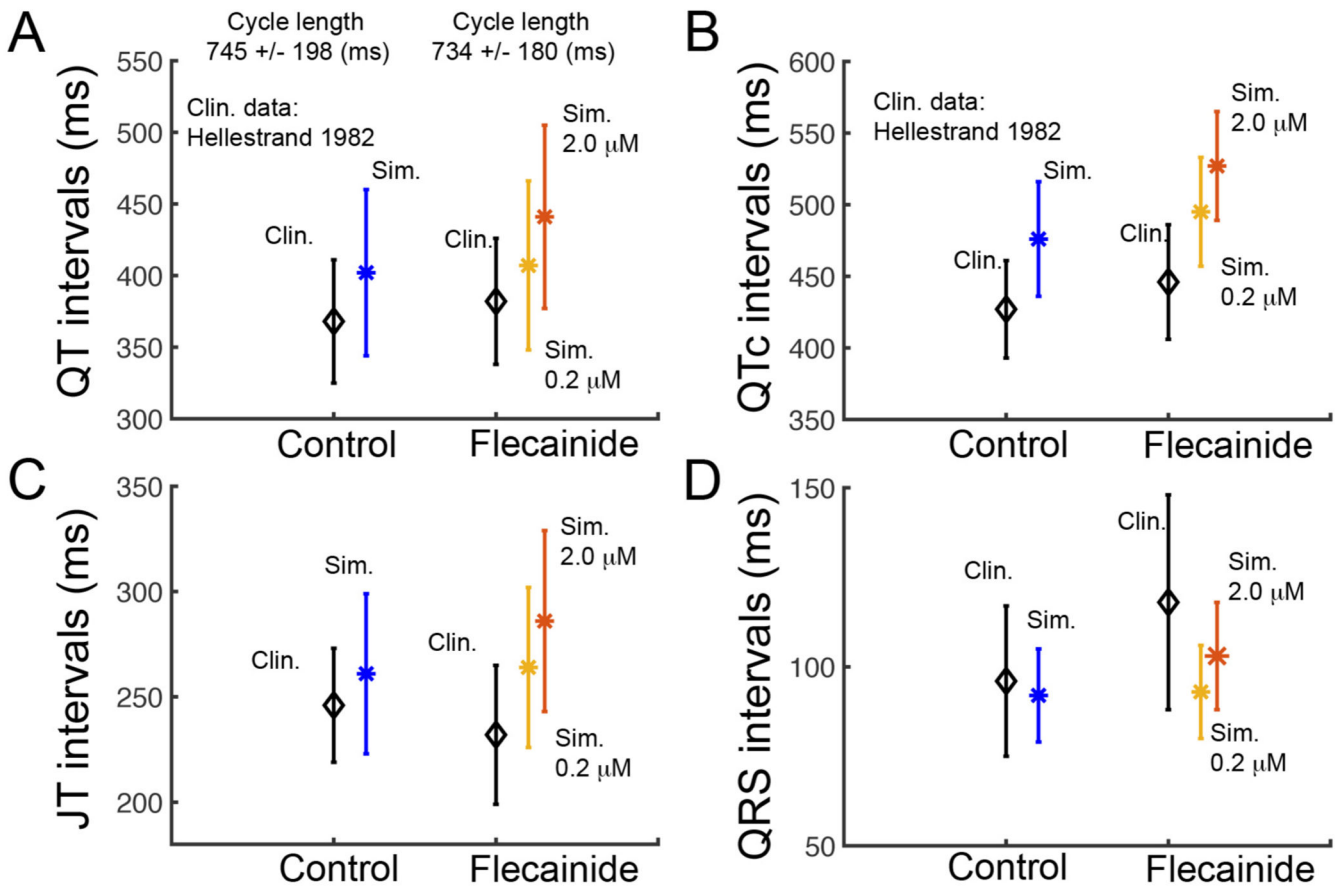
Fig. 2.
Validation of the simulated drugs with human clinical data (A) QT intervals and (B) Heart rate corrected pseudo ECG (QT$_C$ interval) was computed from a 1-dimensional strand of Grandi-Bers human cardiac ventricular myocytes for a range of flecainide concentrations (0.2 and 2.0 μM) compared to clinical data (black lines). (C) Comparison of human clinical data showing control and flecainide affected JT intervals (black lines) and simulated mean values under the same conditions ((yellow and red lines). (D) The clinically observed and in silico prediction of QRS intervals changes in a dose-dependent manner. Clinical data: $n = 39$ for QT, QTc, and JT intervals; $n = 47$ for QRS.
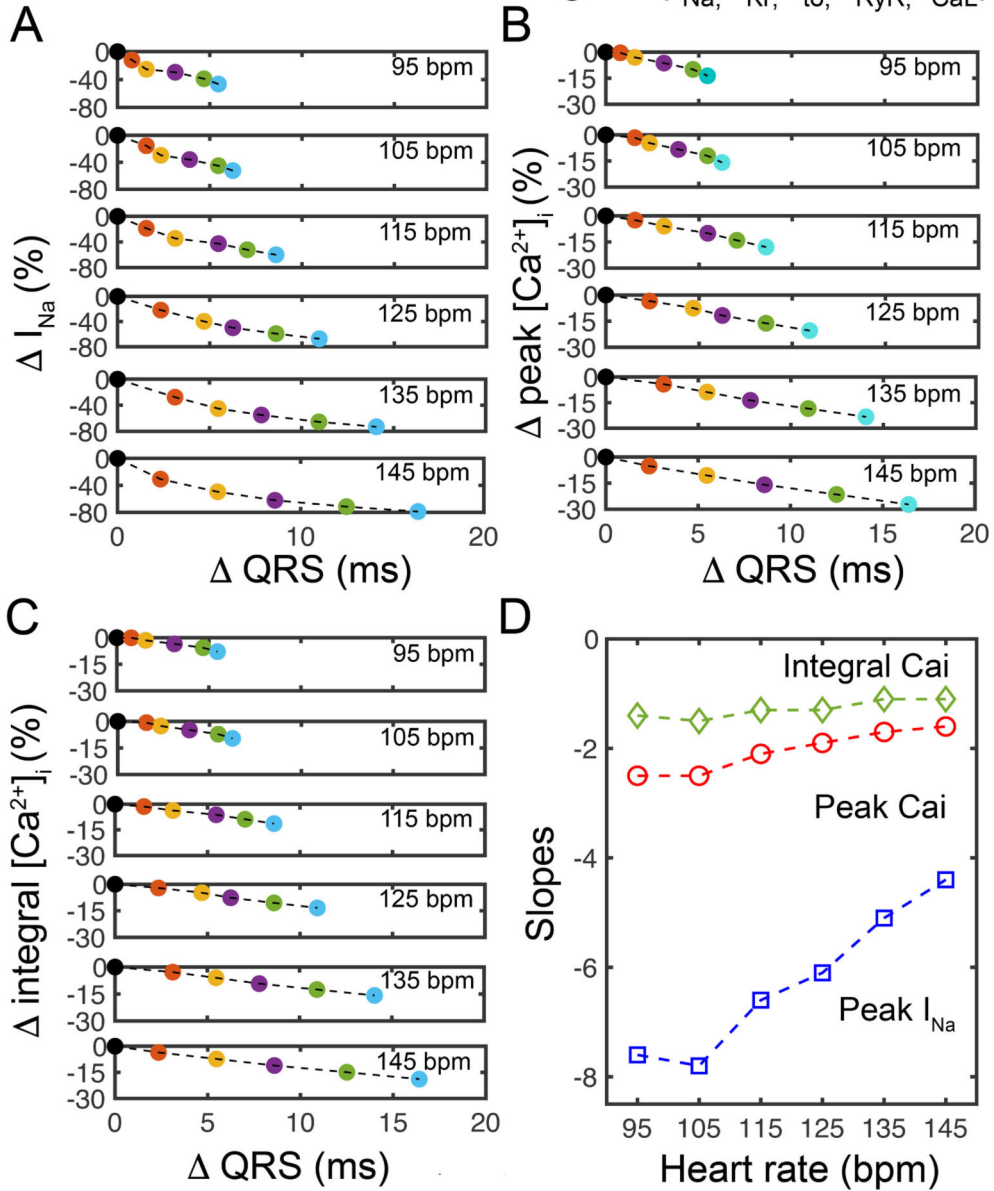
Fig. 3.
Predicted effects of flecainide in human ventricular computational tissue on the relationship between the widening of QRS duration and (A) the peak I_{Na}, and (B) the peak intracellular Ca^{2+} transient, and (C) the integral of the Ca^{2+} transient, and (C) from 0 (drug free – black), 0.5 (red), 1.0 (yellow), 1.5 (purple), 2.0 (green) to 2.5 (blue) μM flecainide with the indicated heart rate from 95 to 145 BPM. (D) Slopes of correlation between the QRS, the peak I_{Na}, peak intracellular Ca^{2+} transient and integral of the Ca^{2+} transient as a function of heart rates.

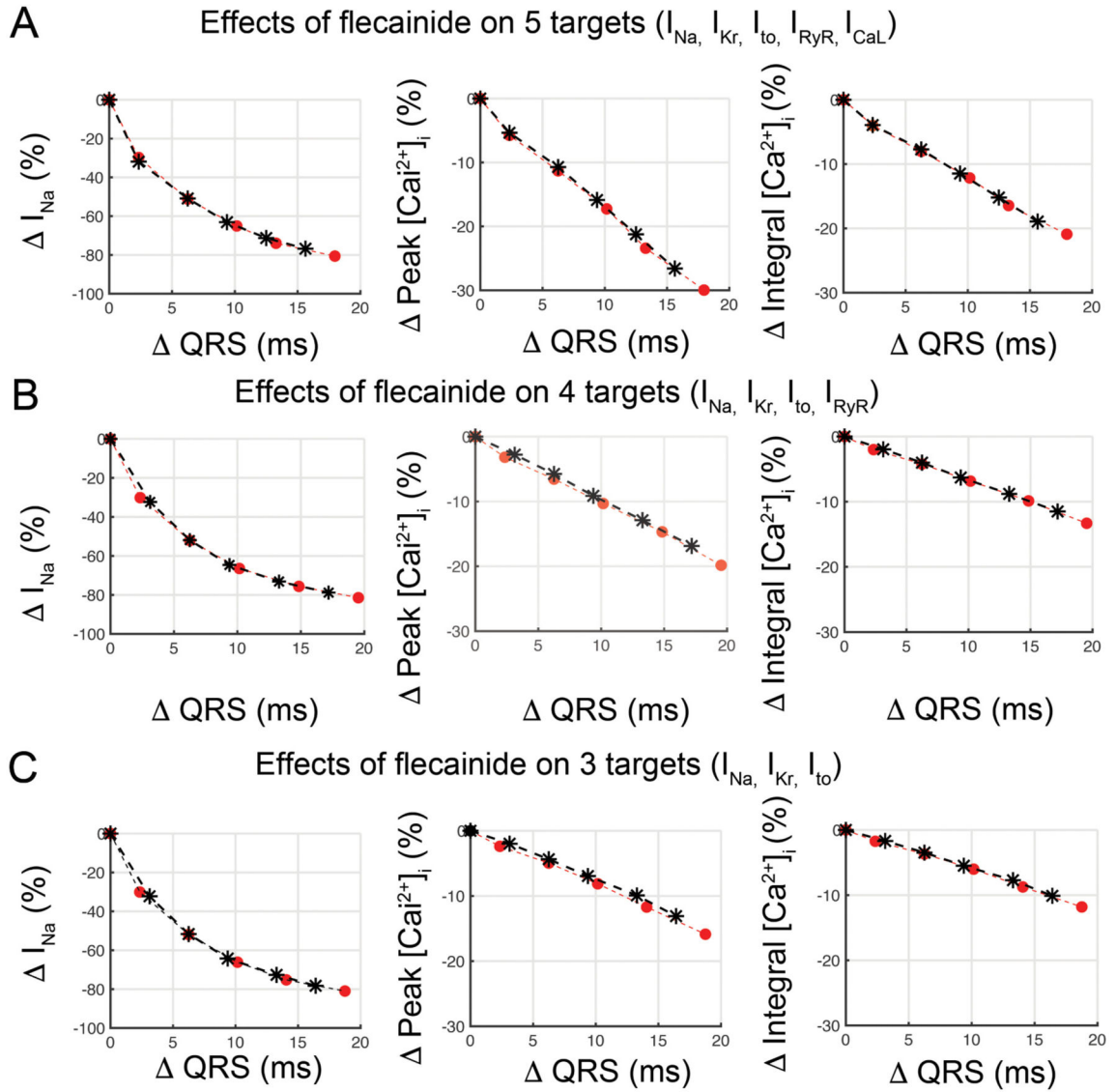5 targets (I_{Na}, I_{Kr}, I_{to}, I_{RyR}, I_{CaL})
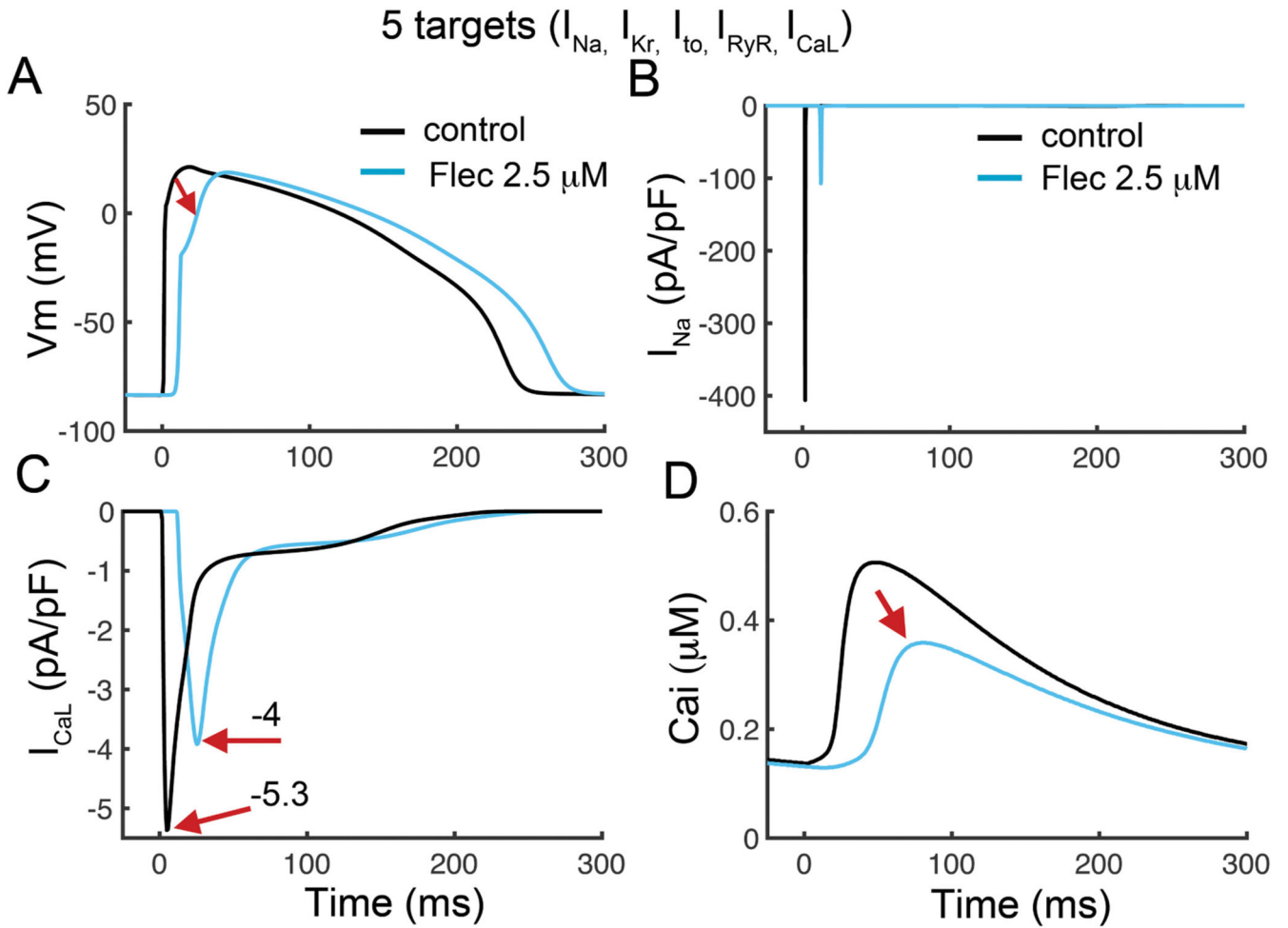
Fig. 4.
Illustration of the ionic mechanisms of simulated effects of flecainide on human ventricular computational tissue on 5 targets: I_{Na}, I_{Kr}, I_{to}, I_{RyR}, I_{CaL}. Fibers of 165 cells were paced at 150 BPM for 1500 beats. (A) The last conducted action potential of the middle cell (cell #82) is shown. (B) 2.5 μM flecainide (blue) reduced peak I_{Na} and depressed cellular excitability (red arrow), as well as (C – D) reduced I_{CaL} activation and the intracellular Ca^{2+} transient.
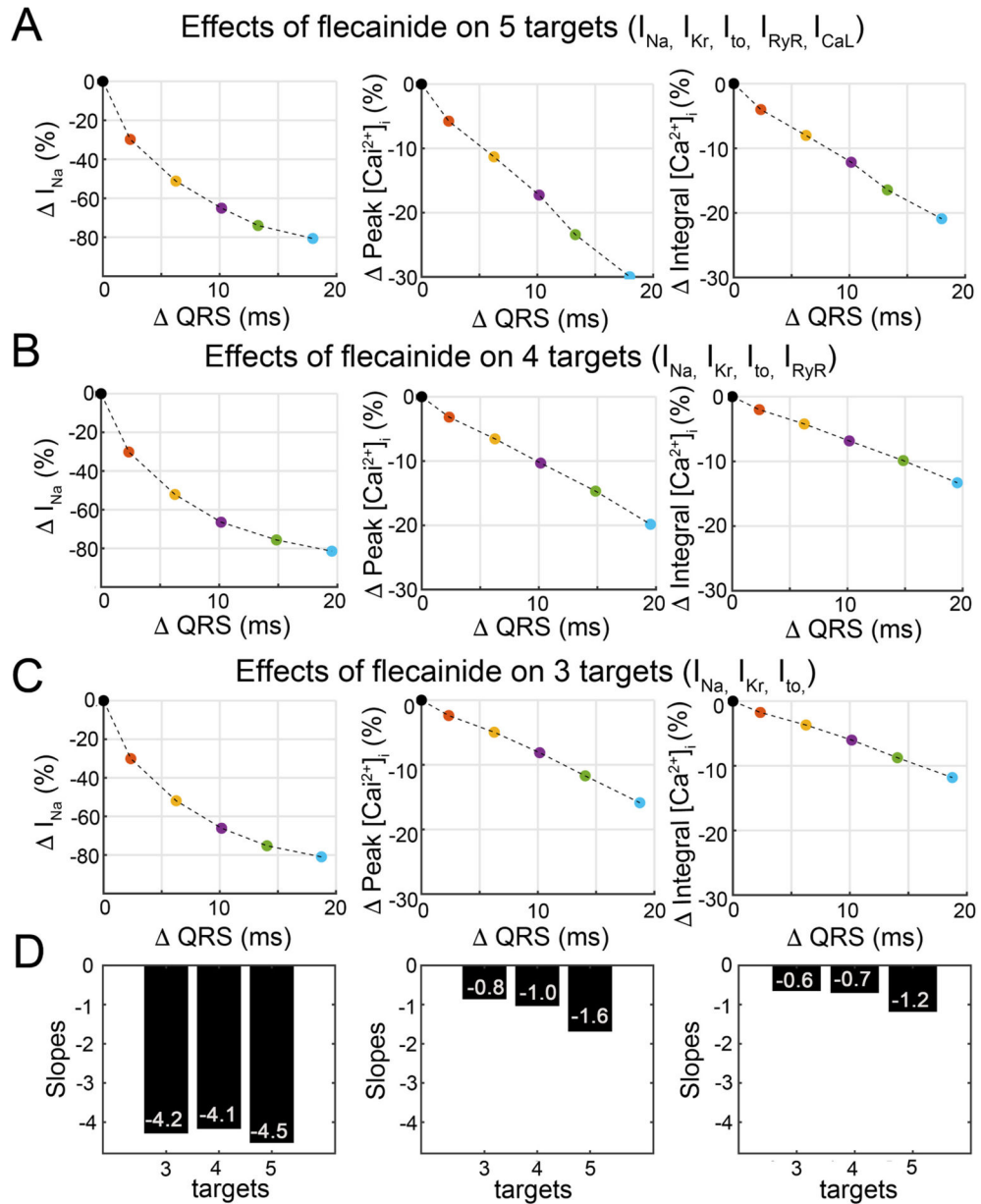
Fig. 5.

Correlation between flecainide-induced widening of simulated human ventricular computational tissue derived QRS and reduction in peak Ca^{2+} transient, and integral of the Ca^{2+} transient, and peak I_{Na} within the therapeutic plasma range of 0.5 to 2.5 μM (0.5 - red, 1.0 - yellow, 1.5 - purple, 2.0 – green and 2.5 – blue). (A) Effects of flecainide on 5 targets, (B) Effects of flecainide on 4 targets and (C) Effects of flecainide on 3 targets. (D) slopes of relationship between flecainide- induced widening of simulated QRS and reduction in peak I_{Na} (left), and peak Ca^{2+} transient (middle) and integral of the Ca^{2+} transient (right) for each case. Fibers of 165 cells were paced at 150 BPM for 1500 beats. The last conducted action potential of the middle cell (cell #82) is shown.
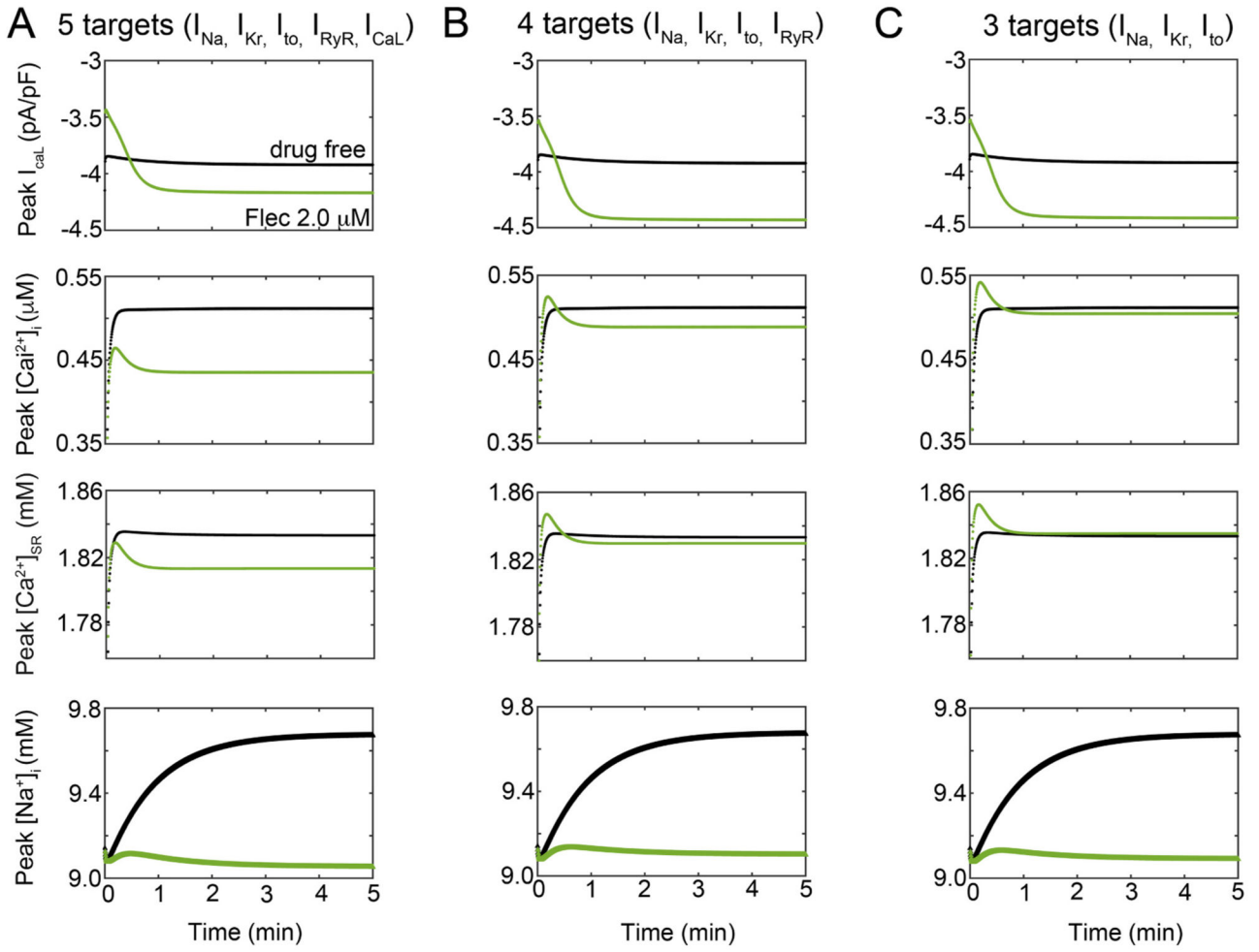
Fig. 6.
Grandi-Bers Human ventricular model: Ionic mechanisms of flecainide effects for 10 mins simulated time at 150 BPM with 2.0 μM flecainide (green) for (A) effects of flecainide on 5 targets, (B) effects of flecainide on 4 targets and (C) effects of flecainide on 3 targets on I_{CaL}, $[Ca^{2+}]_i$, $[Ca^{2+}]_{SR}$ and $[Na^+]_i$.

Fig. 7.
Flecainide-induced widening of simulated QRS from human ventricular computational tissue and reduction in Ca^{2+} transient and I_{Na} at 150 BPM within the therapeutic plasma range of 0.5 to 2.5 μM (red dots) compared with intercellular sodium concentrations fixed at 9.7 mM (black asterisks) for (A) effects of flecainide on 5 targets, (B) effects of flecainide on 4 targets and (C) effects of flecainide on 3 targets.
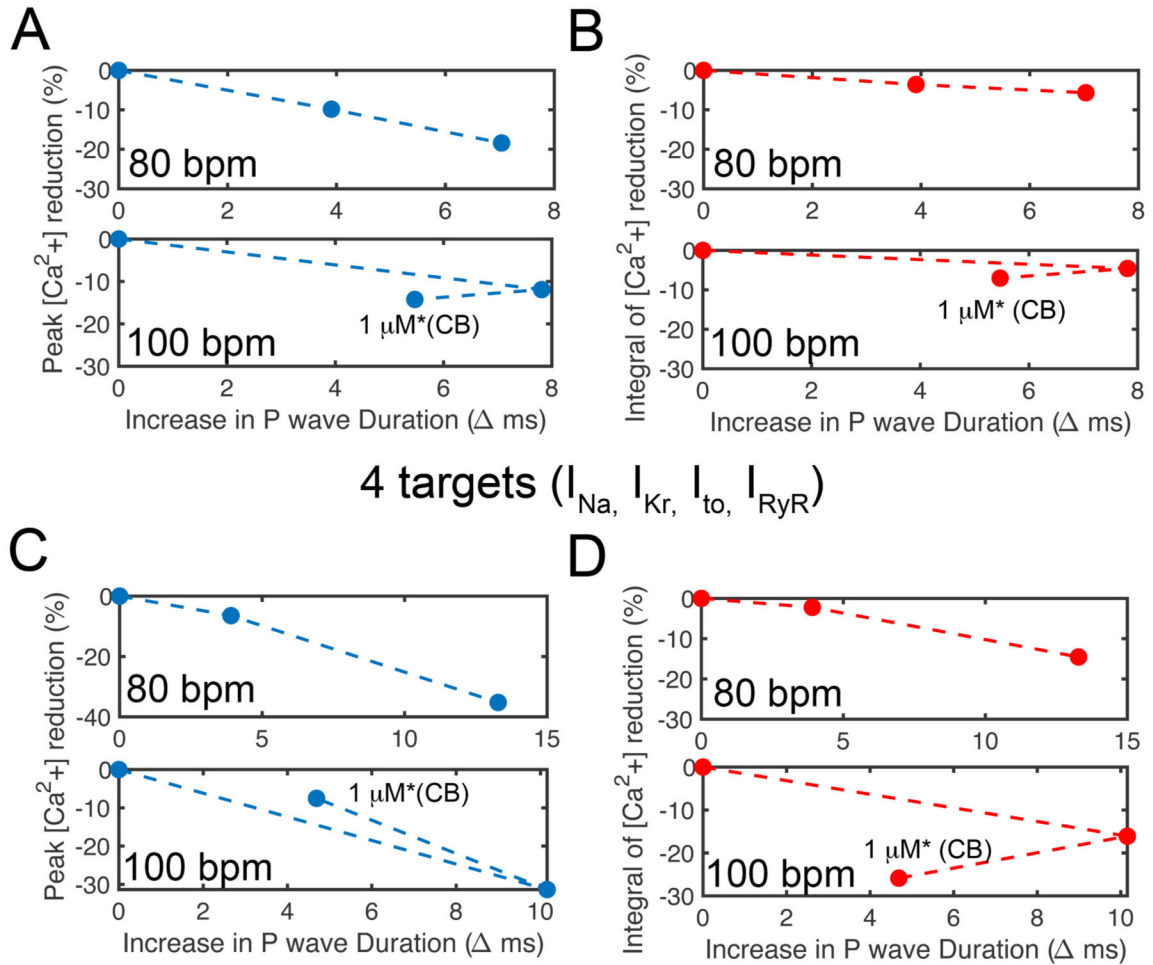
Fig. 8.

Correlation between flecainide-induced widening of P wave in human atrial computational tissue and reduction in the peak intracellular Ca^{2+} transient (blue), and the integral of the Ca^{2+} transient (red) at 80 and 100 BPM with flecainide 0.5 and 1.0 μM. (A) and (B) Simulated effects of flecainide on 5 targets: I_{Na}, I_{Kr}, I_{to}, I_{RyR}, I_{CaL}). (C) and (D) Simulated effects of flecainide on 4 targets: I_{Na}, I_{Kr}, I_{to}, I_{RyR}). Notice that the * indicates that conduction block (CB) occurs at the indicated concentration.